

# RSC Advances



This is an *Accepted Manuscript*, which has been through the Royal Society of Chemistry peer review process and has been accepted for publication.

*Accepted Manuscripts* are published online shortly after acceptance, before technical editing, formatting and proof reading. Using this free service, authors can make their results available to the community, in citable form, before we publish the edited article. This *Accepted Manuscript* will be replaced by the edited, formatted and paginated article as soon as this is available.

You can find more information about *Accepted Manuscripts* in the [Information for Authors](#).

Please note that technical editing may introduce minor changes to the text and/or graphics, which may alter content. The journal's standard [Terms & Conditions](#) and the [Ethical guidelines](#) still apply. In no event shall the Royal Society of Chemistry be held responsible for any errors or omissions in this *Accepted Manuscript* or any consequences arising from the use of any information it contains.

## ARTICLE

# Effective Hydrodechlorination of 4-chlorophenol catalysed by magnetic palladium/reduced graphene oxide under mild conditions

Cite this: DOI: 10.1039/x0xx00000x

Yanlin Ren<sup>a</sup>, Guangyin Fan<sup>a\*</sup>, Weidong, Jiang<sup>b</sup>, Bin Xu<sup>b</sup>, and Fuan Liu<sup>b</sup>,Received 00th January 2012,  
Accepted 00th January 2012

DOI: 10.1039/x0xx00000x

www.rsc.org/

Magnetic palladium/reduced graphene oxide nanocomposites (Pd/rGO-Fe<sub>3</sub>O<sub>4</sub>) were prepared by the depositing Pd nanoparticles on the magnetic support rGO-Fe<sub>3</sub>O<sub>4</sub>. The as-prepared nanocomposites were investigated as catalysts for the hydrodechlorination of 4-chlorophenol in aqueous phase. The complete conversion of 4-chlorophenol (concentration as high as 2.5 g/L) to phenol was obtained in a reaction time of 40 min at room temperature and balloon hydrogen pressure without any additives. The excellent catalytic activity of Pd/rGO-Fe<sub>3</sub>O<sub>4</sub> can be attributed to the small particle size of Pd and an electron-deficient state of Pd in the catalyst as a result of the strong interaction between the active sites and the oxygen of the oxygen containing groups on the support rGO-Fe<sub>3</sub>O<sub>4</sub>.

## 1. Introduction

Chlorinated phenols are valuable chemicals with wide utilization in the field of agriculture and industry. However, the residual chlorinated phenols show significant associations with adverse effects on the environment and human beings due to their high toxicity and resistance to biodegradation.<sup>1</sup> Among the technologies for detoxifying these poisonous pollutants, catalytic hydrodechlorination (HDC) has attracted great attention because this method is recognized as holding high efficiency, performing at relatively mild conditions and yielding reduced toxic products such as phenol, cyclohexanol, and cyclohexanone. Especially, the HDC of chlorinated phenols catalyzed by supported noble metal catalysts through the scission of carbon-chlorine bonds on the metal surface using molecular hydrogen as a hydrogen source is among the most investigated in recent years. Ascribed to the metallic phase, palladium is the subject of intensive researches because of its special activity toward the HDC reaction.<sup>2</sup> However, the HDC activity is always prohibited due to the severe catalyst deactivation caused by the surface adsorption of chlorine from the carbon-chlorine bonds<sup>3</sup> and aggregation of active Pd particles.<sup>4, 5</sup> To overcome these drawbacks, large amount of additives such as bases were introduced into the reaction systems, while extra work are needed to segregate them from the reaction mixture in order to avoid the secondary pollution. Up to now, it still remains a tremendous challenge to seek stable and recyclable catalysts for detoxifying the chlorinated phenols under mild conditions without any additives.

Besides the catalytic nature of metal nanoparticles (NPs) themselves, it has been proposed that the support also plays a critical role in enhancing the catalytic performance of metal catalyst. Bearing

this in mind, a variety of supports including ZrO<sub>2</sub><sup>6</sup>, Al<sub>2</sub>O<sub>3</sub><sup>7-11</sup>, and carbon<sup>4, 5, 11-16</sup> have been investigated and applied in the detoxication of wastewater containing chlorinated phenols. Among these supports, metal oxides can improve the stability of active sites of the catalysts, nevertheless they are more sensitive to HCl produced from the HDC reaction, resulting in loss of catalytic activity. Comparatively, carbon materials as supports are more resistant to acid and thus have intrigued extensive interests of researchers on surveying their usefulness in catalytic decomposing chlorophenols. Activated carbon (AC), as a typical carbon carrier, has been demonstrated with strong ability in uniformly distributing the metal active sites due to its high surface area and porosity. However, the application of AC as a support in the HDC reaction, depending on its pore size distribution and surface composition, may cause the adsorption of substrate as well which results in a poor recycling property. Several additives were also employed to assist these carbon materials for achieving better dispersion of metal NPs and catalytic performance. For example, by modifying the carbon nanofibers with pyridinic basic species via the treatment of carbon nanofibers in a stream of NH<sub>3</sub> gas, Liu et al. have successfully improved the catalytic activity and stability of Pd NPs on carbon nanofibers for the HDC of chlorophenol. However, very high temperature is required to introduce such basic species.<sup>17</sup> Afterwards, Jin and co-workers reported a Pd/MSCN (mesoporous silica-carbon nano-composite) catalyst

which exhibited pronounced activity for the catalytic HDC of 4-CP at room temperature under ordinary hydrogen using triethylamine ( $\text{Et}_3\text{N}$ ) as a base additive.<sup>18</sup> Therefore, it is a big challenge to explore appropriate supports with fine stability in an acidic environment and strong capability to interact with metal catalysts for recyclable conversion of chlorinated phenols under mild conditions without additives.

In a previous work, we found that the catalyst Pd/rGO exhibited excellent performance for the HDC of 4-chlorophenol (4-CP)<sup>19</sup>, however long time centrifugation are required to separate the catalyst. To this end, we prepared the magnetic rGO supported palladium catalyst and applied for the catalytic HDC of 4-CP. The as-prepared catalyst showed excellent catalytic performance with the yield of phenol as a sole product. The catalyst can be isolated from the reaction mixture by an external magnet and can be reused four times without obvious loss of activity.

## 2. Experiment

### 2.1 Materials

$\text{Na}_2\text{PdCl}_4$  was purchased from the Kunming Institute of Precious Metals, China.  $\text{FeCl}_2 \cdot 4\text{H}_2\text{O}$ ,  $\text{FeCl}_3 \cdot 6\text{H}_2\text{O}$  and graphite powder were provided by Chengdu Kelong Chemical Reagent Factory. Other chemicals and solvents (analytical grade reagents) were supplied from the Aladdin Industrial Corporation, China, and used as received without further purification.

### 2.2 Catalyst preparation

The GO used in this procedure was synthesized by the oxidation of graphite according to the improved hummer's method<sup>20</sup>. For the synthesis of rGO- $\text{Fe}_3\text{O}_4$ ,  $\text{FeCl}_2 \cdot 4\text{H}_2\text{O}$  (411 mg) and  $\text{FeCl}_3 \cdot 6\text{H}_2\text{O}$  (1118 mg) were dissolved in deionized water (25 mL). Then, the as-prepared mixture was transferred into a yellow-brown suspension of GO which was firstly prepared through the adding of GO (100 mg) into deionized water (75 mL) under ultrasonication. Immediately, the PH value of the mixture was adjusted to 11 by adding ammonia, and followed by the reduction of the mixture at 363 K for 4 h using hydrazine hydrate (4 mL) as a reducing agent. After cooling down to room temperature, the black solid was washed with water and ethanol several times, and the dried under vacuum at 343 K for 12 h to yield the rGO- $\text{Fe}_3\text{O}_4$ .

The rGO- $\text{Fe}_3\text{O}_4$  stabilized Pd NPs (Pd/rGO- $\text{Fe}_3\text{O}_4$ ) were fabricated as follows: The desired amount of rGO- $\text{Fe}_3\text{O}_4$  (100 mg) and an aqueous solution of  $\text{Na}_2\text{PdCl}_4$  (2.78 mg/mL, 5 mL) were mixed into a 50 mL round-bottom flask under ultrasonication for 30 min. Afterward, the flask was put into an ice-water bath, an aqueous solution of  $\text{NaBH}_4$  (5.6 mg/mL, 5 mL) was slowly added into the above mixture under vigorous stirring. After stirring for 4 h, the black solid was collected with a magnet, washed with deionized water several times, and finally dried under vacuum at 343 K for 12 h. (The content of Pd was 5.0 wt.% estimated by the ICP)

### 2.3 Catalyst characterization

The morphology and particle size of the catalysts were characterized by Transmission electron microscopy (TEM) measurements, which were carried out on a JEOL model 2010 instrument operated at an accelerating voltage of 200 kV. Powder X-ray diffraction (XRD) patterns were recorded on a Rigaku X-ray diffractometer D/max-2200/PC equipped with Cu  $K\alpha$  radiation (40 kV, 20 mA). The samples were scanned over the range of 10-90°. X-ray photoelectron spectroscopy (XPS, Kratos XSAM800) spectra was obtained by using Al  $K\alpha$  radiation (12 kV and 15 mA) as an excitation source ( $h\nu = 1486.6$  eV) and Au (BE Au4f = 84.0 eV) and Ag (BE Ag3d = 386.3 eV) as reference. All binding energy (BE) values were referenced to C1s peak of contaminant carbon at 284.6 eV.

### 2.4 Activity test

The HDC of 4-CP was chosen as a model reaction to estimate the catalytic property of the Pd/rGO- $\text{Fe}_3\text{O}_4$  nanocomposites. Typically, the HDC reaction was conducted in a two-necked round-bottom flask equipped with a hydrogen balloon. The reaction temperature was controlled by a thermal controller. Specifically, an appropriate amount of catalyst (ca. 5.0 mg) and an aqueous solution of 4-CP (ca. 2.5 g/L, 5.0 mL) were transferred into the flask, followed by treating the reactor under vacuum and charging with high pure hydrogen. After that, the reactor was put into the water bath. The stirring rate was adjusted to 1200 rpm and the reaction time was accounted when the setting reaction temperature was achieved. To monitor the process of the HDC reaction, samples were withdrawn from the reactor with a syringe periodically. The removal efficiency of Pd/rGO- $\text{Fe}_3\text{O}_4$  for 4-CP was analyzed by GC (Agilent 7890A) with a FID detector and PEG-20M capillary column (30 m $\times$ 0.25 mm, 0.25  $\mu\text{m}$  film) and nitrogen was used as a carrier gas.

## 3. Results and discussion

### 3.1 Characterization of Pd/RGO- $\text{Fe}_3\text{O}_4$

The particle sizes and morphologies of the rGO- $\text{Fe}_3\text{O}_4$  and Pd/rGO- $\text{Fe}_3\text{O}_4$  nanocomposites were characterized by TEM and the results are illustrated in Fig 1. As shown in Fig. 1a and c, the  $\text{Fe}_3\text{O}_4$  NPs have been successfully immobilized on the surface of rGO with various kinds of shapes such as sphere and quadrilateral. The particle size of the sphere was in the range from about 4 to 15 nm, and the average edge length of the quadrilateral was about 15 nm. From the EDX result, it can be seen that carbon, oxygen and Fe were detected. During the process of depositing Pd NPs on the rGO- $\text{Fe}_3\text{O}_4$ , the smaller spherical  $\text{Fe}_3\text{O}_4$  disappeared and resulted in larger one because of the aggregation of the particle in the progress of the Pd precursor reduction. Interestingly, the Pd NPs were well dispersed not only on the surface of rGO but also on the  $\text{Fe}_3\text{O}_4$  with an average particle size of 1.8 nm and a narrow size distribution of 1.1-2.8 nm (Fig. 1b and d). The EDX

characterization showed that Pd NPs were successfully deposited on the surface of the rGO-Fe<sub>3</sub>O<sub>4</sub> through the reduction of Pd<sup>2+</sup> using NaBH<sub>4</sub> as a reducing agent, which was confirmed by the elemental mapping(Fig.1g).

The XRD patterns of graphite, GO, rGO-Fe<sub>3</sub>O<sub>4</sub> and Pd/rGO-Fe<sub>3</sub>O<sub>4</sub> are shown in Fig. 2. The graphite exhibited a very strong

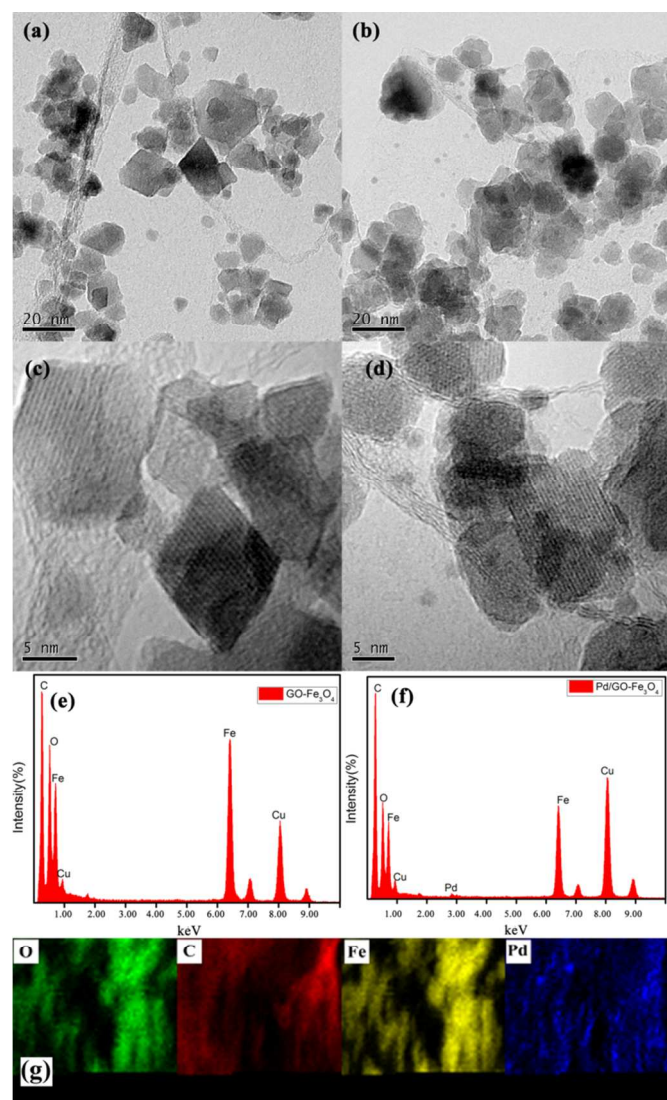


Fig.1 TEM images of rGO-Fe<sub>3</sub>O<sub>4</sub>(a,c) and Pd/rGO-Fe<sub>3</sub>O<sub>4</sub>(b,d); EDX spectrums of rGO-Fe<sub>3</sub>O<sub>4</sub>(e) and Pd/rGO-Fe<sub>3</sub>O<sub>4</sub>(f); Elemental mapping of Pd/rGO-Fe<sub>3</sub>O<sub>4</sub>(g)

and sharp peak at 26.4° which was assigned to the (002) crystal plane of graphite. As can be observed, such diffraction peak disappeared and accompanied by the appearance of a new peak at 10.0° after the oxidation of graphite to GO. This phenomenon was possibly attributed to the insertion of various oxygen-containing functional groups (epoxy, hydroxyl, carboxyl and carbonyl) between the layer of the GO.<sup>21</sup> As shown in Fig.2c, this peak eventually removed though the treatment of GO and iron precursors using hydrazine hydrate as the reducing agent. Meantime, the peaks located at 30.1°, 35.5°,

43.1°, 53.5°, 57.0°, and 62.6° matched well with (220), (311), (400), (422), (511), and (440) Bragg diffractions of Fe<sub>3</sub>O<sub>4</sub> (JCPDS no. 76-0956) respectively, confirming the formation of Fe<sub>3</sub>O<sub>4</sub> crystalline phase. However, the weak peaks at 32.9 and 49.3° which was attributed to the hematite were also detected<sup>22</sup>, resulting in an impurity of the sample, nevertheless the presence of hematite also can enhance the magnetic property of the catalyst to some extent. A new peak at 40.1° which belonged to the (111) Bragg diffraction of Pd (JCPDS no. 88-2335) demonstrated the successful immobilization of palladium on the support of rGO-Fe<sub>3</sub>O<sub>4</sub>.

XPS profiles of GO and Pd/rGO-Fe<sub>3</sub>O<sub>4</sub> were documented and illustrated in Fig.3. XPS survey scan performed on the sample GO showed that the existence of oxygen and carbon on the surface of the GO sheets. The C1s spectrum is deconvoluted into four peaks at 284.5, 285.5, 287.0 and 288.3 eV (Fig. 3a) which are attributed to the C-C, C-OH, C-O-C and HO-C=O

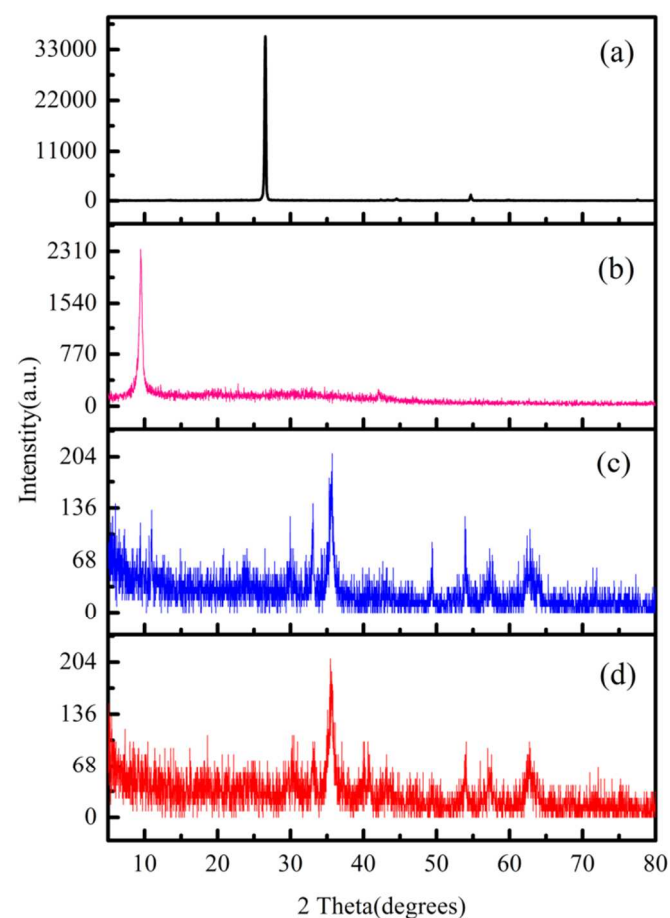


Fig.2 XRD patterns of graphite (a), GO (b), rGO-Fe<sub>3</sub>O<sub>4</sub>(c) and Pd/rGO-Fe<sub>3</sub>O<sub>4</sub> (d)

groups, respectively<sup>21</sup>. In case of Pd-RGO-Fe<sub>3</sub>O<sub>4</sub>, apart from carbon and oxygen, iron and palladium were distinctively observed. Compared to the C1s spectrum of GO, it can be seen that the peak intensities for oxygen-containing functionalities are substantially reduced, indicating that GO was successfully reduced during the procedure. Especially, it should be noted that the peak corresponding to C-O-C groups disappeared and



resulted in an enhancement of the intensity of the C-C groups. The residue of the hydroxyl groups such as OH and COOH on the surface of the catalyst not only improves the hydrophilicity of the catalyst but also stabilizes the Pd NPs as anchoring sites, ensuring the fine dispersion of the Pd NPs on rGO-Fe<sub>3</sub>O<sub>4</sub>.

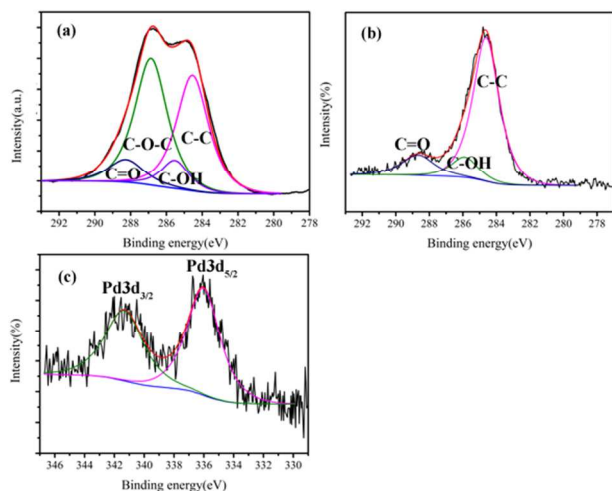


Fig.3 XPS spectrums of GO (a), rGO-Fe<sub>3</sub>O<sub>4</sub> (b) and Pd/rGO-Fe<sub>3</sub>O<sub>4</sub>(c)

As shown in Fig.3c, the XPS spectrum of Pd was also characterized to ascertain the oxide state of Pd. As can be observed, the Pd binding energy of Pd/rGO-Fe<sub>3</sub>O<sub>4</sub> showed two strong peaks centered at 341.3 and 336.0 eV, which were attributed to the Pd3d<sub>3/2</sub> and Pd3d<sub>5/2</sub> peaks respectively, indicating that the Pd<sup>2+</sup> has been completely reduced during the process. However, it should be noted that the metallic Pd was in an electron-deficient state since the binding energy of Pd 3d<sub>3/2</sub> was 0.6 eV higher than the standard spectrum, which was ascribed to the reduction of electron density of Pd atoms caused by the interaction between the metallic Pd phase and the high electronegativity of oxygen of the oxygen containing groups in GO. Interestingly, the electro-deficient Pd were supposed to be responsible for the improving catalytic performance of the catalysts for HDC reaction<sup>3,23</sup>, which was approved by the excellent catalytic activity of the Pd/rGO-Fe<sub>3</sub>O<sub>4</sub> at room temperature and balloon hydrogen pressure in our work.

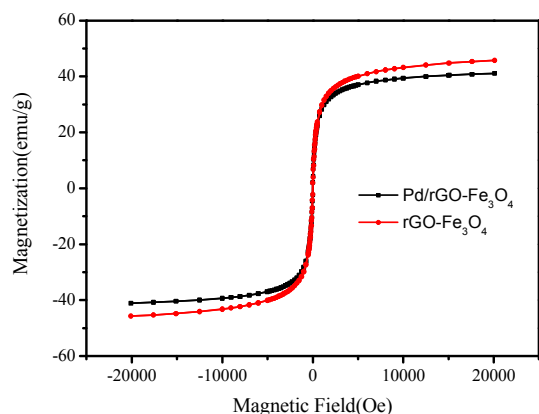


Fig.4 Room temperature magnetization curves of rGO-Fe<sub>3</sub>O<sub>4</sub> and Pd/rGO-Fe<sub>3</sub>O<sub>4</sub>

Magnetic properties of the samples rGO-Fe<sub>3</sub>O<sub>4</sub> and Pd/rGO-Fe<sub>3</sub>O<sub>4</sub> were also investigated and the hysteresis loops of rGO-Fe<sub>3</sub>O<sub>4</sub> and Pd/rGO-Fe<sub>3</sub>O<sub>4</sub> are illustrated in Fig.4. It can be seen that the magnetic saturation value of the rGO-Fe<sub>3</sub>O<sub>4</sub> was 91.4 emu/g, while the value decreased to 82.2 emu/g due to the immobilization of Pd NPs on the surface of the support in agreement with the literature reported by Ma et al.<sup>8</sup> However, the decrease of the saturation magnetization did not affect the separation of the catalyst from the reaction system, since the catalyst can be easily separated from the reaction mixture by a magnet.

### 3.2 Catalytic properties of Pd/rGO-Fe<sub>3</sub>O<sub>4</sub>

Table 1 Hydrodechlorination of chlorophenols catalyzed by different catalysts

Catalysts	Time (min)	Substrates	Conversion (%)	Selectivity (%)
rGO	25	4-CP	-	-
rGO-Fe <sub>3</sub> O <sub>4</sub>	25	4-CP	-	-
Pd/rGO	25	4-CP	99.8	99.0
Pd/rGO-Fe <sub>3</sub> O <sub>4</sub>	25	4-CP	100.0	99.2
Pd/rGO-Fe <sub>3</sub> O <sub>4</sub>	30	2-CP	100.0	99.5
Pd/rGO-Fe <sub>3</sub> O <sub>4</sub>	20	3-CP	100.0	98.1
Pd/rGO-Fe <sub>3</sub> O <sub>4</sub>	40	2,4-DCP	100.0	>99.8
Pd/rGO-Fe <sub>3</sub> O <sub>4</sub>	50	2,6-DCP	100.0	99.9
Pd/rGO-Fe <sub>3</sub> O <sub>4</sub>	120	2,4,6-TCP	100.0	99.9

Reaction conditions: catalyst, 5.0 mg; Temperature, 303 K; pressure, 1atm; solvent, water (2.5 g/L, substrate concentration).

The HDC of 4-CP was chosen as a model reaction to investigate the catalytic property of the catalyst Pd/rGO-Fe<sub>3</sub>O<sub>4</sub>. Except the main product phenol, only a trace amount of cyclohexanol and cyclohexanone were detected during the reaction process. From the results listed in Table 1, it can be seen that no conversion of 4-CP was observed using rGO or

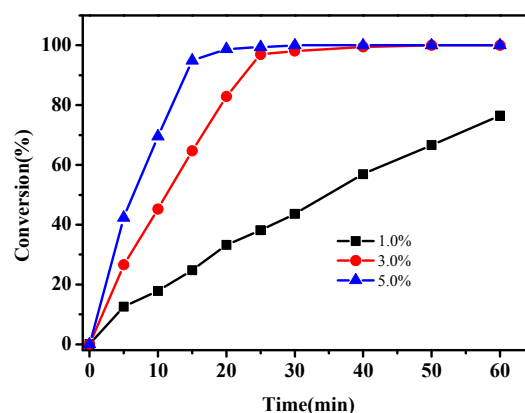


Fig.5 Effect of Pd loading on the HDC of 4-CP catalyzed by Pd/rGO-Fe<sub>3</sub>O<sub>4</sub>.

rGO-Fe<sub>3</sub>O<sub>4</sub> as a catalyst at 303 K and balloon hydrogen pressure, indicating that Pd was the active sites for the HDC of 4-CP. For comparison, the Pd/rGO catalyst without magnetic

property was also prepared and used for the HDC reaction. It exhibited a comparable activity compared with the catalyst Pd/rGO-Fe<sub>3</sub>O<sub>4</sub> towards HDC of 4-CP, however high speed centrifugation are required to separate the catalyst from the reaction mixture due to its hydrophilicity of the Pd/rGO ascribed to the functional groups of oxygen containing groups on the surface of rGO. Therefore, the nanocomposite Pd/rGO-Fe<sub>3</sub>O<sub>4</sub> was chosen as the catalyst for HDC.

Effect of catalyst loading on the catalytic performance of the catalyst Pd/rGO-Fe<sub>3</sub>O<sub>4</sub> was firstly investigated at 303 K and balloon hydrogen pressure. From the results illustrated in Fig.5, it can be seen that the conversion of 4-CP to phenol increased with the elevation of Pd loading. Specifically, the time for complete conversion of 4-CP was 50 and 30 min when the Pd loading was 3.0 wt.% and 5.0 wt.% respectively, while only 76.4 conversion of 4-CP was obtained in 60 min with a Pd loading of 1.0 wt.%. Therefore, 5 wt.% loading of Pd was selected to further investigate the catalytic property of the catalyst Pd/rGO-Fe<sub>3</sub>O<sub>4</sub> towards the HDC of 4-CP.

Effect of catalyst concentration on the HDC efficiency over the catalyst Pd/rGO-Fe<sub>3</sub>O<sub>4</sub> was studied with the variation of catalyst concentration from 0.5 to 1.5 g/L and the results are shown in Fig.6. One can see that the conversion of 4-CP increased with the increase of catalyst concentration. For instance, the conversion of 4-CP was 93.7 % in 60 min with a low catalyst concentration of 0.5 g/L. To our surprise, a complete conversion of 4-CP to phenol was achieved in 30 min when the catalyst concentration was 1.0 g/L. The reaction time for complete conversion of 4-CP was 15 min when the catalyst concentration was increased to 1.5 g/L. Ascribed to the product distributions, the increase of catalyst concentration did not change the final product in which phenol was detected as the main product. Therefore, the catalyst concentration was set to 1.0 g/L to further investigate other factors that affected the catalytic performance of the catalyst Pd/rGO-Fe<sub>3</sub>O<sub>4</sub>.

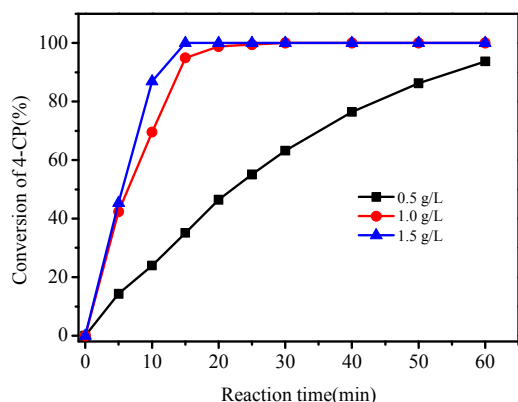


Fig.6 Effect of catalyst dosage on the HDC of 4-CP catalyzed Pd/rGO-Fe<sub>3</sub>O<sub>4</sub>

Effect of 4-CP concentration on the catalytic HDC of 4-CP over catalyst Pd/rGO-Fe<sub>3</sub>O<sub>4</sub> was explored. As shown in Fig.7, the increase of 4-CP concentration led to a decrease of

conversion rate. The conversion of 4-CP was accomplished at a short reaction time of 15 and 20 min when the concentration of 4-CP was 1.5 and 2.0 g/L respectively. The reaction time for complete conversion of 4-CP increased to 25 and 40 min when 2.5 and 3.0 g/L of 4-CP was introduced to the reaction system. Moreover, the change of 4-CP concentration did not affect the product distributions since only phenol was observed with the increase of 4-CP concentration from 1.5 to 3.0 g/L. Consequently, the catalytic HDC of 4-CP catalyzed by our Pd/rGO-Fe<sub>3</sub>O<sub>4</sub> catalyst holds the high activity under mild conditions without any additives.

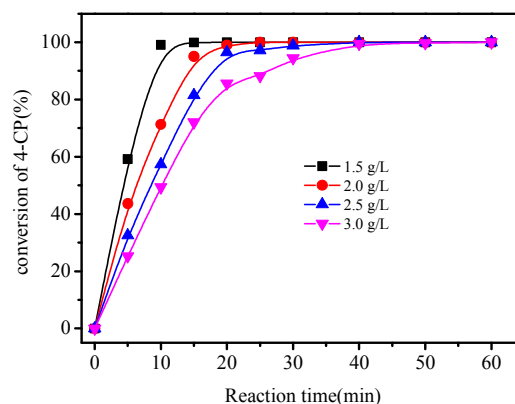


Fig.7 Effect of 4-CP concentration on the catalytic performance of the catalyst Pd/rGO-Fe<sub>3</sub>O<sub>4</sub>

Effect of temperature on the catalytic property of the catalyst Pd/rGO-Fe<sub>3</sub>O<sub>4</sub> was investigated under different temperatures keeping other reaction parameters the same and the results are illustrated in Fig.8. As expected, the conversion of 4-CP increased gradually with the elevation of reaction temperature from 293 to 308 K. In term of the selectivity, the product distributions did not change obvious in the investigated temperatures. It has been reported that the catalytic HDC of 4-

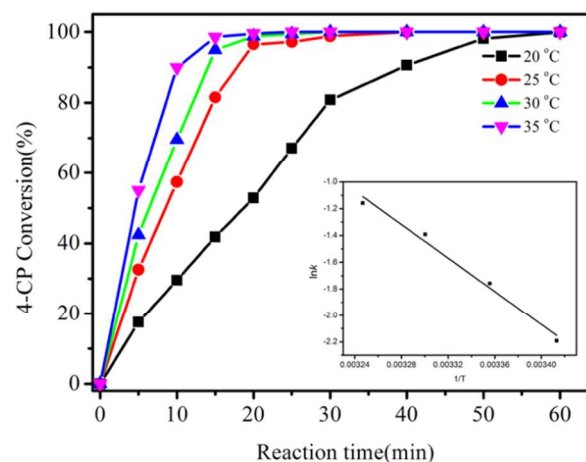


Fig.8 Effect of reaction temperature on the HDC of 4-CP over the catalyst Pd/rGO-Fe<sub>3</sub>O<sub>4</sub>

CP was a pseudo-first-order reaction. Thus, the activation energy for the HDC of 4-CP with the use of Pd/rGO-Fe<sub>3</sub>O<sub>4</sub> as a catalyst can be evaluated. According to the Arrhenius equation as follow,

$$k_{obs} = Ae^{-E_a/RT}$$

the activation energy ( $E_a$ ) was calculated. In the equation,  $k_{obs}$  represents the estimated first-order rate constant,  $A$  reveals the frequency factor,  $R$  and  $T$  express the ideal gas constant and temperature, respectively. As shown in Fig.9, the rate constants originated from the slope of the straight line were 0.1118, 0.1725, 0.2488, and 0.3138 at 293, 298, 303, and 308 K respectively. The coefficient of determination ( $R^2$ ) values was  $>0.99$  in all tests. Consequently, the activation energy for the HDC of 4-CP over the catalyst Pd/rGO-Fe<sub>3</sub>O<sub>4</sub> is approximately  $52.0 \pm 4.2$  kJ/mol.

As reported from the previous literature, solvent plays an important role in the catalytic property of the catalyst as well as the product distributions of the HDC reaction.<sup>24, 25</sup> To this end, different solvents such as water, ethanol, *i*-propanol, methanol, HF and hexane were introduced to test the catalytic property of the catalyst Pd/rGO-Fe<sub>3</sub>O<sub>4</sub> and the results are illustrated in Fig 7. It was observed that the initial reaction rate of 4-CP was followed the order: water > methanol > ethanol > *i*-propanol > THF > hexane. Especially, the HDC of 4-CP achieved as high as 100 % within 40 min in water under the same reaction conditions. When water was replaced by the protic solvents such as methanol, ethanol and *i*-propanol, the conversion of 4-CP were obviously decreased and even lower 4-CP conversion were observed in aprotic solvents such as THF and hexane. It was reported that dielectric constant ( $\epsilon$ ) and molar volume ( $v$ ) are two of the most important properties which can affect the catalytic performance of the catalyst in the HDC reaction. For example, the initial rate for the HDC of 2,4-DCP can be influenced by the solvent polarity and structure which was

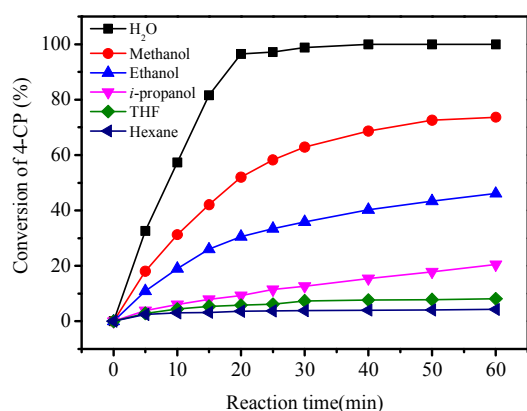


Fig.9 Effect of solvents on the HDC of 4-CP over catalyst Pd/rGO-Fe<sub>3</sub>O<sub>4</sub>

corresponded to the dielectric constant( $\epsilon$ ) and molar volume( $v$ ).<sup>24</sup> The initial rate of 2, 4-DCP was promoted with the increased strength in the ionic forces because of the solvation. On the other hand, a lower molar volume of the

solvent enables more solvent molecular to interact with the charge reaction intermediate and strengthened the HDC reaction.<sup>24</sup> Especially, the solvent water has the highest/lowest values of  $\epsilon$  and  $v$ , which can form well organized structures through the formation of an H-bonding between the dissolving ions exhibiting the highest catalytic activity for HDC reaction. The solvents such as THF and hexane with a lower solvation ability and H-bonding (if any) or without these properties reached a lower catalytic activity.<sup>24</sup> Similarly, our results discussed above confirmed the argument. Therefore, a higher value of  $\epsilon$ , a lower value of  $v$  and molar volume should be taken into consideration to achieve a higher reaction rate.

We also investigated the catalytic performance of the catalyst Pd/rGO-Fe<sub>3</sub>O<sub>4</sub> and the results are shown in Table 1. It can be seen that the complete conversions of 3-CP, 2-CP, and 4-CP could be accomplished in different reaction time due to the electronic and steric hindrance of the substrates. Moreover, the catalyst also showed excellent catalytic properties for the HDC of dichlorophenols (2,4-DCP and 2,6-DCP) and trichlorophenol (2,4,6-TCP) with the increase of reaction time. Under the same conditions, the HDC rate follows the order: monochlorophenols > dichlorophenols > trichlorophenol. The reusability of the catalyst was also investigated. As shown in Fig.10, the results indicate that the catalyst was quite stable and can be recycled for four times without the loss of any activity. Moreover, the catalyst can be easily separated from the reaction medium with a magnet and the Pd leaching was negligible analyzed by ICP ( $<0.1\%$ ). Such phenomenon proved the good stability of Pd/rGO-Fe<sub>3</sub>O<sub>4</sub> for the catalytic HDC of 4-CP. The excellent catalytic properties of Pd/rGO-Fe<sub>3</sub>O<sub>4</sub> were probably attributed to the following reasons. Firstly, the electron-deficient state of Pd, which was caused by the interaction between the metallic Pd and the oxygen of the oxygen containing groups in rGO,

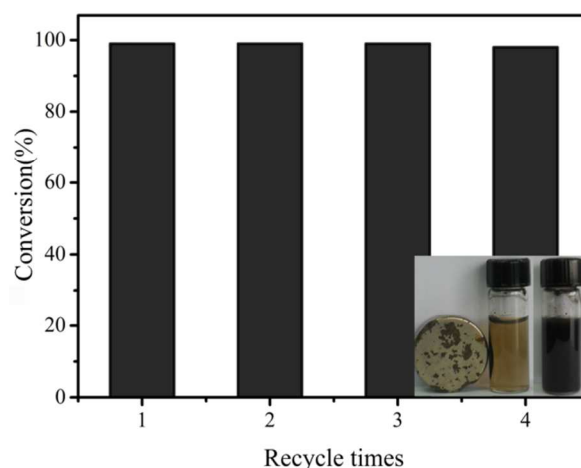


Fig.10 Reusability of the catalyst Pd/rGO-Fe<sub>3</sub>O<sub>4</sub>

plays an important role in improving the catalytic property of the catalyst towards the HDC of the chlorinated compounds in agreement with the reported literature<sup>9, 26</sup>. Moreover, a smaller Pd particle size was more tolerable to the HCl during the HDC process. Finally, the magnetic property of the catalyst was

easily recycled in a facile collection of catalysts and immune from the loss usually caused by a mechanical recycling. This advanced composite material provides a kind of novel and effective catalyst with great promise for catalytic HDC of 4-CP in practical application.

#### 4. Conclusion

In summary, the catalyst Pd/rGO-Fe<sub>3</sub>O<sub>4</sub> was synthesized and applied for the HDC of 4-CP in aqueous phase at room temperature and balloon hydrogen pressure. Through the characterization, it can be seen that the Pd NPs were of narrow size distribution and dispersed well on the surface of the magnetic support rGO-Fe<sub>3</sub>O<sub>4</sub>. The results indicated that the magnetic catalyst Pd/rGO-Fe<sub>3</sub>O<sub>4</sub> showed excellent catalytic property for 4-CP HDC. The high catalytic activity could be attributed to the smaller particle size of Pd combined with the functional groups on the surface of rGO, which resulted in an electron-deficient of Pd from the strong metal-support interaction and the presence of hydroxyl groups on the surface of the support. Furthermore, the catalyst exhibited quite stable property and can be recycled at least four times without significant deactivation. It was easily separated from the reaction mixture without filtration due to the magnetic property of the catalyst.

#### Acknowledgements

This work was financially supported by the National Natural Science Foundation of China (21207109), the Applied Basic Research Programs of Science and Technology Department of Sichuan Province (No. 2014JY0107), and the Opening Project of Key Laboratory of Green Catalysis of Sichuan Institutes of High Education (No. LZJ1205)

#### Notes and references

<sup>a</sup> Chemical Synthesis and pollution control Key Laboratory of Sichuan Province, college of chemistry and Chemical Industry, China West Normal University, Nanchong 637009, P. R.China.

<sup>b</sup> Key Laboratory of Green Catalysis of Sichuan Institute of High Education, Zigong 643000, P. R. China

1. M. A. Keane, *ChemCatChem*, 2011, **3**, 800-821.
2. H. Rong, S. Cai, Z. Niu and Y. Li, *ACS Catalysis*, 2013, **3**, 1560-1563.
3. J. A. Baeza, L. Calvo, M. A. Gilarranz and J. J. Rodriguez, *Chem. Eng. J.*, 2014, **240**, 271-280.
4. P. Albers, J. Pietsch and S. F. Parker, *J. Mol. Catal. A: Chem.*, 2001, **173**, 275-286.
5. C. Xia, Y. Liu, S. Zhou, C. Yang, S. Liu, J. Xu, J. Yu, J. Chen and X. Liang, *J. Hazard. Mater.*, 2009, **169**, 1029-1033.
6. Y. Shao, Z. Xu, H. Wan, H. Chen, F. Liu, L. Li and S. Zheng, *J. Hazard. Mater.*, 2010, **179**, 135-140.
7. S. Srinivas, P. S. Prasad and P. K. Rao, *Catal. Lett.*, 1998, **50**, 77-82.
8. F. Zhang, J. Jin, X. Zhong, S. Li, J. Niu, R. Li and J. Ma, *Green Chemistry*, 2011, **13**, 1238-1243.
9. C. B. Molina, A. H. Pizarro, J. A. Casas and J. J. Rodriguez, *Appl. Catal., B* 2014, **148-149**, 330-338.
10. G. Yuan and M. A. Keane, *Appl. Catal., B* 2004, **52**, 301-314.
11. Z. M. de Pedro, E. Diaz, A. F. Mohedano, J. A. Casas and J. J. Rodriguez, *Appl. Catal., B* 2011, **103**, 128-135.

12. A. Wiersma, E. Van de Sandt, M. Makkee, C. Luteijn, H. Van Bekkum and J. Moulijn, *Catal. Today* 1996, **27**, 257-264.
13. R. Nie, J. Wang, L. Wang, Y. Qin, P. Chen and Z. Hou, *Carbon*, 2012, **50**, 586-596.
14. Y. Mitoma, M. Kakeda, A. M. Simion, N. Egashira and C. Simion, *Environ. Sci. Technol.*, 2009, **43**, 5952-5958.
15. L. Calvo, M. A. Gilarranz, J. A. Casas, A. F. Mohedano and J. J. Rodriguez, *J. Hazard. Mater.*, 2009, **161**, 842-847.
16. G. Yuan and M. A. Keane, *Catal. Commun.*, 2003, **4**, 195-201.
17. Q. Liu, Z.-M. Cui, Z. Ma, S.-W. Bian and W.-G. Song, *J. Phys. Chem. C*, 2008, **112**, 1199-1203.
18. Z. Jin, C. Yu, X. Wang, Y. Wan, D. Li and G. Lu, *J. Hazard. Mater.*, 2011, **186**, 1726-1732.
19. H. Deng, G. Fan, C. Wang and L. Zhang, *Catal. Commun.*, 2014, **46**, 219-223.
20. D. C. Marcano, D. V. Kosynkin, J. M. Berlin, A. Sinititskii, Z. Sun, A. Slesarev, L. B. Alemany, W. Lu and J. M. Tour, *ACS nano*, 2010, **4**, 4806-4814.
21. F. Urbano and J. Marinas, *J. Mol. Catal. A: Chem.*, 2001, **173**, 329-345.
22. X. Liang, X. Wang, J. Zhuang, Y. Chen, D. Wang and Y. Li, *Adv. Funct. Mater.*, 2006, **16**, 1805-1813.
23. C. Molina, A. Pizarro, J. Casas and J. Rodriguez, *Appl. Catal., B* 2014, **148**, 330-338.
24. S. Gómez-Quero, E. Díaz, F. Cárdenas-Lizana and M. A. Keane, *Chem. Eng. Sci.*, 2010, **65**, 3786-3797.
25. S. Gómez-Quero, F. Cárdenas-Lizana and M. A. Keane, *AIChE J.*, 2010, **56**, 756-767.
26. L. M. Gómez-Sainero, X. L. Seoane, J. L. G. Fierro and A. Arcoya, *J. Catal.*, 2002, **209**, 279-288.